NJC

PAPER

View Article Online
View Journal | View Issue

Cite this: *New J. Chem.*, 2016, **40**, 1230

Detailed studies of the interaction of 3-chloroaniline with *O,O′*-diphenylphosphoryl-isothiocyanate†

Maria G. Babashkina,* Koen Robeyns, Yaroslav Filinchuk and Damir A. Safin

Received (in Montpellier, France) 23rd September 2015,
Accepted 9th November 2015

DOI: 10.1039/c5nj02588e

www.rsc.org/njc

The reaction of neat 3-chloroaniline with neat S═C═N–P(O)(OPh)$_2$ leads to a new *N*-phosphorylated thiourea, 3-ClC$_6$H$_4$NHC(S)NHP(O)(OPh)$_2$ (**1**). The same reaction in non-dried CH_2Cl_2 or C_6H_6 leads to the salt-like compounds [3-ClC$_6$H$_4$NH$_3$]$^+$[NCS]$^-$ (**2**) and [3-ClC$_6$H$_4$NH$_3$]$^+$[P(O)$_2$(OPh)$_2$]$^-$·0.5C$_6$H$_6$ (**3·0.5C$_6$H$_6$**), respectively, while using non-dried acetone yields 1-(3-chlorophenyl)-4,4,6-trimethyl-3,4-dihydropyrimidine-2(1*H*)-thione (**4**). Dissolution of **1** in non-dried CH_2Cl_2, C_6H_6 or Me_2C═O leads to the direct formation of **2**, **3·0.5C$_6$H$_6$** and **4**, respectively. It was established that thione **4** is most likely formed through the thiourea **1**-assisted aldol condensation of acetone leading to mesityl oxide. In turn the latter ketone interacts with **1** followed by its hydrolysis leading to **4**. Compounds **1–4** have been characterized by NMR spectroscopy and elemental analysis and their molecular structures were elucidated by X-ray diffraction. Hirshfeld surface analysis showed that the structures of both **1** and **4** are mainly characterized by H···H, H···C, H···Cl and H···S contacts as well as by H···O in the structure of **1**. The enrichment ratio, derived as the decomposition of the crystal contact surface between pairs of interacting chemical species, for **1** was found, as expected for the polar contacts, which are generally hydrogen bonds, to be significantly larger than unity for the contacts of the type H···O and H···S. A much larger than unity value was found for the enrichment ratio of the C···C contacts in the structure of **1**, which is due to extensive π···π stacking in the crystal packing. The enrichment ratio for **4** was found to be larger than unity for the contacts of the type H···C and, but with a lesser degree, H···Cl and H···S.

Introduction

We have extensively studied the synthesis, membrane transport, extraction, separation and complexation properties of *N*-(thio)phosphorylated thioureas R^{1}R^{2}NC(S)NHP(X)(OR^3)$_2$ (**NTTUs**) (R^1, R^2 = H, alkyl, aryl; R^3 = iPr, Ph; X = O, S), which are readily obtained by reacting primary or secondary amines with the corresponding *N*-(thio)phosphorylated isothiocyanate (Scheme 1).[1] The crucial influence of the R^{1}R^{2}N function has been established for the behavior of thioureas in solution as well as their complexation properties. On the other hand, an overwhelming majority of the reported **NTTUs** contains the OiPr functions at the phosphoryl group, while only two examples, RNHC(S)NHP(O)(OPh)$_2$ (R = iPr, Ph),[1s,w] were reported for the OPh-containing derivatives. Notably, it was found that the recrystallization of

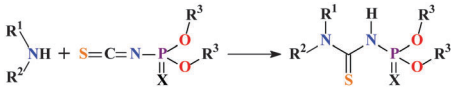

Scheme 1 Synthesis of **NTTUs** (R^1, R^2 = H, alkyl, aryl; R^3 = iPr, Ph; X = O, S).[1]

iPrNHC(S)NHP(O)(OPh)$_2$ from aqueous Me_2C═O leads to the formation of a salt-like compound [iPrNH$_3$]$^+$[P(O)$_2$(OPh)$_2$]$^-$.[1s] This is most likely due to a strong influence of the electron withdrawing OPh groups at the P═O group leading to the weakening of the P–N bond. Nothing similar was observed for OiPr-containing **NTTUs**.

On the other hand, multicomponent reactions are of ever increasing interest and importance in chemistry for the production of, *e.g.*, organic and medicinal products of value.[2] The main advantage of multicomponent reactions over conventional ones is that three or more components act together in a single reaction allowing us to avoid possible time consuming processes. This becomes even more crucial for drug discovery.[3] Moreover, the synthetic strategy based on multicomponent reactions allows us to vary and tune the structure of the target product in a broad range. For example, the Biginelli

Institute of Condensed Matter and Nanosciences, Université catholique de Louvain, Place L. Pasteur 1, 1348 Louvain-la-Neuve, Belgium.
E-mail: maria.babashkina@gmail.com

† Electronic supplementary information (ESI) available: Crystallographic data (including CIF files), selected bond distances and angles, hydrogen bonds and π···π stacking interactions. CCDC 1423371–1423374. For ESI and crystallographic data in CIF or other electronic format see DOI: 10.1039/c5nj02588e

dihydropyrimidine synthesis, the so-called "Biginelli condensation",[4] is a one-pot three component reaction, which is a powerful tool to produce dihydropyrimidine-2-thiones.[5] This is a relatively novel class of compounds, which is of great importance due to their pharmacological activities such as antibacterial,[6] antitumour,[7] antioxidative,[8] analgesic and anti-inflammatory properties.[5,9] Furthermore, dihydropyrimidine-2-thiones were found to be efficient antihypertensive agents as well as calcium channel blockers and neuropeptide Y antagonists.[10]

In continuation of our comprehensive studies of the **NTTU** ligands, we have directed our attention to new *N*-phosphorylated thiourea 3-$ClC_6H_4NHC(S)NHP(O)(OPh)_2$ (**1**), containing OPh functions at the phosphoryl group as well as the functionalised arylamine fragment at the thiocarbonyl group. Herein, we report the detailed studies on the solvent-influenced interaction of 3-chloroaniline with *N*-phosphorylated isothiocyanate S═C═N–P(O)$(OPh)_2$.

Results and discussion

Synthesis

The reaction of neat 3-chloroaniline with neat S═C═N–P(O)$(OPh)_2$ leads to new *N*-phosphorylated thiourea **1** (Scheme 2). Surprisingly, the same reaction in non-dried CH_2Cl_2 or C_6H_6 under ambient conditions leads to salt-like compounds $[3\text{-}ClC_6H_4NH_3]^+[NCS]^-$ (**2**) and $[3\text{-}ClC_6H_4NH_3]^+[P(O)_2(OPh)_2]^-\cdot 0.5C_6H_6$ (**3·0.5C$_6$H$_6$**), respectively, while using non-dried acetone yields 1-(3-chlorophenyl)-4,4,6-trimethyl-3,4-dihydropyrimidine-2(1*H*)-thione (**4**) (Scheme 2). It was also established that dissolution of **1**, with an initial aim of crystallization, in non-dried CH_2Cl_2, C_6H_6 or Me_2C═O under ambient conditions leads to the direct formation of **2**, **3·0.5C$_6$H$_6$** and **4**, respectively (Scheme 2).

NMR spectroscopy

The $^{31}P\{^1H\}$ NMR signal of freshly dissolved **1** and **3·0.5C$_6$H$_6$** in acetone-d_6 appears as a singlet at −10.5 and −11.7 ppm, respectively. The former signal is in the area characteristic of neutral RNHC(S)NHP(O)$(OPh)_2$ (R = iPr, Ph).[1s,w] The ^{1}H NMR spectra of **1–4** in the same solvent each contain a multiplet signal for the aryl protons at 6.90–7.81 ppm. The ^{1}H NMR spectrum of **1** also contains four broad singlets at 10.97, 12.24, 13.72 and 13.91 ppm, with the former two peaks corresponding to the NHP protons, while the latter two are due to the arylNH protons. The NH_3 protons in the spectra of **2** and **3·0.5C$_6$H$_6$** are shown as a broad singlet at about 8.15 ppm. The ^{1}H NMR spectrum of **4** exhibits a singlet and a doublet at 1.39 and 1.54 ppm, respectively, for the CH_3 protons, while the CH proton of the dihydropyrimidine ring was found as a quartet at 5.00 ppm. Additionally, the spectrum of **4** also contains a broad singlet at 7.90 ppm for the NH proton.

We have further used NMR spectroscopy to study the interaction of **1** with CD_2Cl_2, C_6D_6 and acetone-d_6, each containing a few drops of D_2O. It was found that the $^{31}P\{^1H\}$ NMR spectra of **1** in the former two solvents contain a singlet at about −11.4 ppm, characteristic of the $[P(O)_2(OPh)_2]^-$ anion. This singlet appears after about 3 h and its intensity gradually increases over the next 2–3 days accompanied by the decrease of the $^{31}P\{^1H\}$ NMR signal of **1** till it completely disappears. This process is also accompanied by the appearance of a broad singlet at about 8.05 ppm, characteristic of the NH_3 protons. Thus, thiourea **1** exhibits the same decomposition pathway both in CD_2Cl_2 and C_6D_6. However, the former solvent is favorable for crystallization of the $[NCS]^-$ anion-containing derivative **2**, while the latter solvent supports the formation of the $[P(O)_2(OPh)_2]^-$ anion-containing compound **3**, probably due to efficient co-crystallization with the solvent molecules.

Much more complex results are observed upon dissolution **1** in acetone-d_6. Immediately after dissolution, the $^{31}P\{^1H\}$ NMR spectrum contains a singlet corresponding to the starting thiourea and a singlet at −7.9 ppm, most likely corresponding to the thiourea species with the pronounced negative charge formation on the phosphorylamide nitrogen atom. This is, probably, due strong hydrogen bonding between the NHP hydrogen atom and the oxygen atom of the solvent, which is further supported by the relatively strong acidic nature of the NHP proton[11] induced by strong electron withdrawing arylNHC(S) and P(O)$(OPh)_2$ groups. Furthermore, the $^{31}P\{^1H\}$ NMR spectrum of the completely deprotonated thiourea **1**, which was obtained as its potassium salt K[3-$ClC_6H_4NHC(S)NP(O)(OPh)_2$] by reacting with KOH, contains a singlet at −6.8 ppm, also indicating a low-field shift of the phosphorus signal upon deprotonation. After a few hours a third singlet, characteristic of the $[P(O)_2(OPh)_2]^-$ anion, appears. The intensity of the thiourea signal gradually decreases, while the intensity of the signal at −7.9 ppm increases and then decreases with the constantly increasing signal of the $[P(O)_2(OPh)_2]^-$ anion. Finally, the $^{31}P\{^1H\}$ NMR spectrum contains a unique singlet of the phosphate anion.

As it was mentioned above, the ^{1}H NMR spectrum of freshly dissolved **1** in acetone-d_6 exhibits four broad singlets at 10.97, 12.24, 13.72 and 13.91 ppm, with the former two peaks corresponding to the NHP protons, while the latter two is due to the arylNH protons. The signals at 10.97 and 13.72 correspond to the PNH and arylNH protons, respectively, of the same major

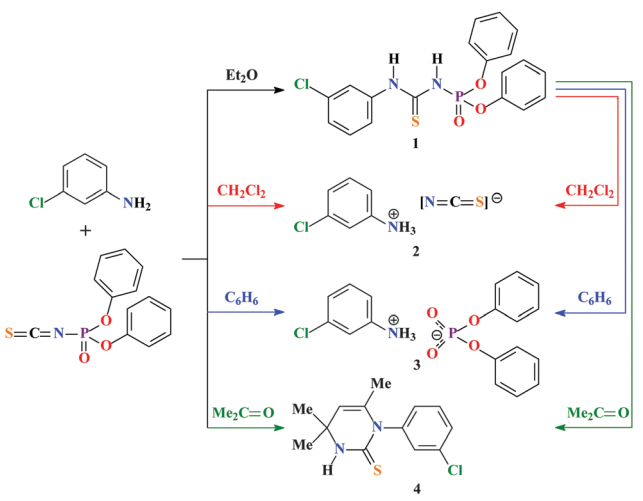

Scheme 2 Synthesis of **1–4**.

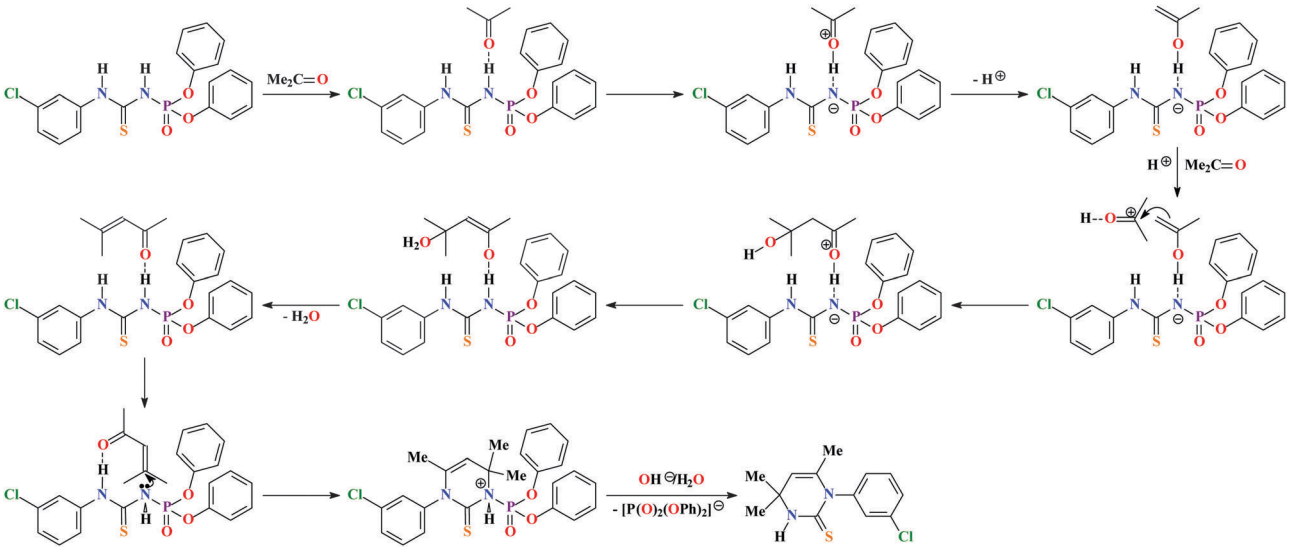

Scheme 3 Probable mechanism of the reaction of **1** with acetone.

species, while the remaining two signals are due to the corresponding NH protons of the other minor species. This was supported by the ratio of their integral intensities. It should be noted that all signals of the NH protons are significantly low field shifted due to strong hydrogen bonding with the solvent molecules. After a few hours the NH signals, corresponding to the major species, decrease, while the signals for the minor species increase and then gradually decrease. Finally, all these singlets completely disappear and a new broad singlet at 7.96 appears. The chemical shift of the latter peak is characteristic of the NH proton of **4**.

Thus, the signal for the NHP proton, being also acidic, exhibits a pronounced low field shift upon involving in hydrogen bonding with acetone-d_6. We can tentatively suggest that acetone undergoes the aldol condensation, which is catalyzed by the acidic NHP proton of **1**, with the formation of mesityl oxide. The latter product further reacts with **1** yielding **4**, accompanied by the hydrolysis of the starting thiourea within the N–P bond (Scheme 3). This hypothesis requires additional in-depth studies, which are currently under progress. However, it was also established that dissolution of **1** in mesityl oxide also leads to the formation of **4**.

Crystal structures

According to X-ray data, **1** and **2**, measured at 150(2) K, and **4**, measured at 297(2) K, crystallize in the monoclinic $P2_1/c$ space group, while **3·0.5C$_6$H$_6$**, measured at 297(2) K, crystallize in the triclinic $P\bar{1}$ space group, respectively. One of the phenyl rings in the structure of **1** is disordered over two positions with a 64% to 36% ratio.

The parameters of the C═S, C–N, P–N and P═O bonds observed for **1** are in the typical range for **NTTU**s (Table S1 in the ESI†).[1] The S═C–N–P═O backbone in the crystal phase has a *cis* conformation (Fig. 1). The crystal structure of **1** is stabilized by intermolecular bifurcated hydrogen bonds of the aryl N–H···O═P and PN–H···O═P types (Fig. 1 and Table S5 in the ESI†). As a result of these hydrogen bonds, 1D polymeric chains are formed (Fig. 1). The structure of **1** is further stabilized by intermolecular π···π stacking interactions with an interplanar separation of about 3.7 Å (Table S6 in the ESI†), formed between the corresponding aromatic rings of adjacent molecules.

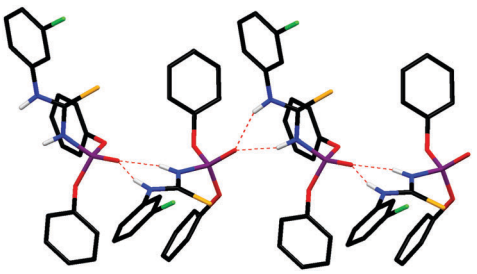

Fig. 1 View on the hydrogen bonded 1D chain in the structure of **1** (hydrogen atoms not involved in H-bonding and disordered phenyl rings are omitted for clarity). Color code: C = black, H = light grey, Cl = green, N = blue, O = red, P = violet, S = orange.

The structure of **2** comprises the $[3\text{-}ClC_6H_4NH_3]^+$ cations and $[NCS]^-$ anions (Fig. 2). The thiocyanate anion is essentially planar with the S–C–N angle being about 179°, and the C═N and C═S bond lengths close to double bonds (Table S2 in the ESI†). Molecules of **2** form 1D polymeric chains, which are constructed due to a net of intermolecular hydrogen bonds between the hydrogen atoms of the NH_3 group of the cation, and the N and S atoms, corresponding to three neighbouring anions (Fig. 2 and Table S5 in the ESI†). As a result of H-bonds, ten-membered heterocycles are formed (Fig. 2).

The crystal structure of **3·0.5C$_6$H$_6$** was found to be a co-crystallization product of $[3\text{-}ClC_6H_4NH_3]^+[P(O)_2(OPh)_2]^-$ and benzene. The P–OPh and P···O bond lengths in the structure of **3·0.5C$_6$H$_6$** indicate a single and intermediate between single and double bonds, respectively (Table S3 in the ESI†). Molecules of **3·0.5C$_6$H$_6$** form 1D polymeric chains, which are constructed due to a net of intermolecular hydrogen bonds between the

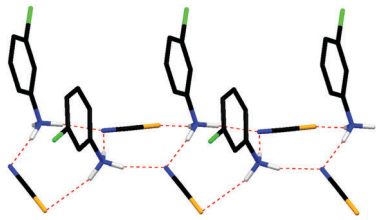

Fig. 2 View on the hydrogen bonded 1D chain in the structure of **2** (hydrogen atoms not involved in H-bonding are omitted for clarity). Color code: C = black, H = light grey, Cl = green, N = blue, S = orange.

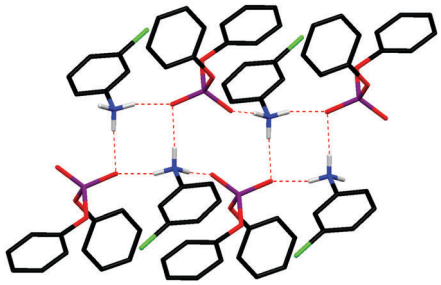

Fig. 3 View on the hydrogen bonded 1D chain in the structure of **3·0.5(C_6H_6)** (hydrogen atoms not involved in H-bonding and benzene molecules are omitted for clarity). Color code: C = black, H = light grey, Cl = green, N = blue, O = red, P = violet, S = orange.

hydrogen atoms of the NH_3 group of the cation and the P···O oxygen atoms, corresponding to three neighbouring anions (Fig. 3 and Table S5 in the ESI†). As a result of H-bonds, eight- and twelve-membered heterocycles are formed (Fig. 3). The structure of **3·0.5C_6H_6** is additionally stabilized by intermolecular π···π stacking interactions with an interplanar separation of about 3.8 Å (Table S6 in the ESI†).

The dihydropyrimidine ring of **4** is in an envelope conformation and is essentially planar with a maximum deviation of 0.115 (4) Å for the carbon atom bearing two methyl substituents (Fig. 4). The C=S bond length indicates a double bond (Table S4 in the ESI†). The two six-membered rings in the structure of **4** are almost orthogonal that is reflected in the corresponding torsion angles (Fig. 4, Table S4 in the ESI†). The crystal packing of **4** is characterized by centrosymmetric dimers connected by N–H···S hydrogen bonds (Fig. 4, Table S5 in the ESI†).

Hirshfeld surface analysis

In order to examine the interactions in the crystal structures of **1** and **4**, the Hirshfeld surface analysis[12] and the 2D fingerprint plots[13] were obtained using CrystalExplorer 3.1.[14]

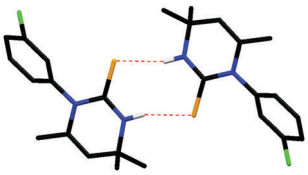

Fig. 4 View on the hydrogen bonded dimer in the structure of **4** (hydrogen atoms not involved in H-bonding are omitted for clarity). Color code: C = black, H = light grey, Cl = green, N = blue, S = orange.

According to the Hirshfeld surface analysis, for **1** and **4** the intermolecular H···H contacts, comprising 43.0 and 51.4% of the total number of contacts, respectively, are major contributors to the crystal packing (Fig. 5, Table 1). The shortest H···H contacts are shown in the fingerprint plots of **1** and **4** as characteristic spikes at $d_e + d_i \approx 1.7$ and 2.6 Å, respectively (Fig. 5). Furthermore, a subtle feature is evident in the fingerprint plot of **1** and it was also significantly less visible in the corresponding plot of **4**. In each of these cases there is a splitting of the short H···H fingerprint. This splitting occurs when the shortest contact is between three atoms, rather than for a direct two-atom contact.[13]

The structures of **1** and **4** are also dominated by C···H contacts, comprising 19.3 and 14.2%, respectively, of the total Hirshfeld surface areas (Table 1). These contacts in both fingerprint plots are shown in the form of clearly pronounced "wings" with the shortest $d_e + d_i \approx 2.7$ Å (Fig. 5), which are recognized as characteristic of a C–H···π interaction.[13] It is worth adding that the fingerprint plot of **1** exhibits a significant number of points at large d_e and d_i, shown as tails at the top right of the plot (Fig. 5). These points, similar to those observed in the fingerprint plot of benzene[13] and phenyl-containing compounds,[15] correspond to regions on the Hirshfeld surface without any close contacts to nuclei in adjacent molecules.

The structure of **4** is further characterized by a significant proportion of H···Cl and H···S contacts, comprising 16.3 and 14.8%, respectively, while a lower proportion (8.8 and 8.5%, respectively) of the same contacts was found in the structure of **1** (Table 1). The structure of **1** exhibits also a pronounced amount of H···O contacts, comprising 11.6% of the total Hirshfeld surface area (Table 1). The shortest H···O and H···S contacts in the fingerprint plots of **1** and **4** are shown as a pair of sharp spikes at $d_e + d_i \approx 1.8$ and 2.5 Å, respectively (Fig. 5). These contacts correspond to the N–H···O (Fig. 1 and Table S5 in the ESI†) and N–H···S (Fig. 4 and Table S5 in the ESI†) hydrogen bonds, respectively. The structure of **1** is further characterized by a proportion of C···C contacts, comprising 3.8% (Table 1). They are shown on the fingerplot as the area of pale blue color on the diagonal at $d_e = d_i \approx 1.8$–1.9 Å (Fig. 5). These contacts correspond to the presence of π···π stacking interactions in the crystal structure of **1** (Table S6 in the ESI†).

Close inspection of other intermolecular contacts also revealed a negligible proportion of C···Cl, Cl···N, Cl···O,

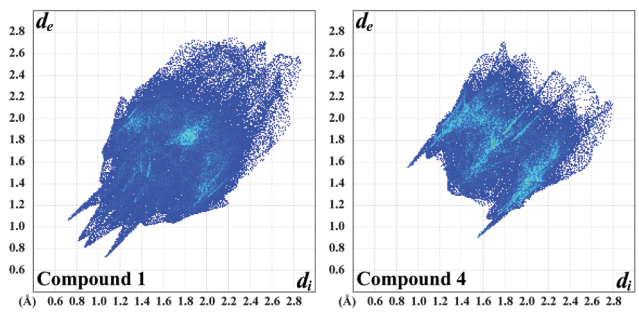

Fig. 5 2D fingerprint plots of observed contacts for **1** and **4**.

Table 1 Hirshfeld contact surfaces and derived "random contacts" and "enrichment ratios" for **1** and **4**. Values are obtained from CrystalExplorer 3.1.[14] The enrichment ratios were not computed when the "random contacts" were lower than 0.9%, as they are not meaningful.[16] The disordered part in the structure of **1** is omitted for clarity; however, its contribution is negligible

	1							**4**				
	H	C	N	Cl	O	P	S	H	C	N	Cl	S
Contacts (C, %)												
H	43.0	—	—	—	—	—	—	51.4	—	—	—	—
C	19.3	3.8	—	—	—	—	—	14.2	0.0	—	—	—
N	0.2	0.1	0.0	—	—	—	—	1.0	0.0	0.0	—	—
Cl	8.8	1.9	1.2	0.0	—	—	—	16.3	0.0	0.0	0.2	—
O	11.6	0.4	0.0	0.7	0.1	—	—	—	—	—	—	—
P	0.0	0.0	0.0	0.0	0.0	0.0	—	—	—	—	—	—
S	8.5	0.0	0.0	0.4	0.0	0.0	0.0	14.8	0.0	0.0	2.2	0.0
Surface (S, %)												
	67.2	14.7	0.8	6.5	6.5	0.0.	4.3	74.6	7.1	0.5	9.5	8.5
Random contacts (R, %)												
H	45.2	—	—	—	—	—	—	55.7	—	—	—	—
C	19.8	2.2	—	—	—	—	—	10.6	0.5	—	—	—
N	1.1	0.2	0.0	—	—	—	—	0.7	0.1	0.0	—	—
Cl	8.7	1.9	0.1	0.4	—	—	—	14.2	1.3	0.1	0.9	—
O	8.7	1.9	0.1	0.8	0.4	—	—	—	—	—	—	—
P	0.0	0.0	0.0	0.0	0.0	0.0	—	—	—	—	—	—
S	5.8	1.3	0.1	0.6	0.6	0.0	0.2	12.7	1.2	0.1	0.8	0.7
Enrichment (E)												
H	0.95	—	—	—	—	—	—	0.92	—	—	—	—
C	0.97	1.73	—	—	—	—	—	1.34	—	—	—	—
N	0.18	—	—	—	—	—	—	—	—	—	—	—
Cl	1.01	1.0	—	—	—	—	—	1.15	0.0	—	0.2	—
O	1.33	0.21	—	—	—	—	—	—	—	—	—	—
P	—	—	—	—	—	—	—	—	—	—	—	—
S	1.47	0.0	—	—	—	—	—	1.17	0.0	—	—	—

C···O, Cl···S, H···N, C···N and O···O contacts in the structure of **1**; and Cl···S, H···N and Cl···Cl contacts in the structure of **4** (Table 1).

We have also determined the enrichment ratios (E)[16] of the intermolecular contacts for **1** and **4** to study the propensity of two chemical species to be in contact. The enrichment ratio, derived from the Hirshfeld surface analysis, is defined as the ratio between the proportion of actual contacts in the crystal and the theoretical proportion of random contacts. E is larger than unity for pair of elements with a higher propensity to form contacts, while pairs which tend to avoid contacts yield an E value lower than unity.

The H···H contacts are favoured in the structures of both **1** and **4** since the enrichment ratios E_{HH} are close to unity and generate an overwhelming majority (43.0 and 51.4% for **1** and **4**, respectively) of the interaction surface (Table 1). The E_{CH}, E_{ClH} and E_{CCl} values of the structure of **1** are also very close to unity, while the former two values of the structure of **4** are even more pronounced (Table 1). The E_{ClH} and E_{CCl} values are the result of abundant S_H (67.2 and 74.6% for **1** and **4**, respectively) proportion of hydrogen atoms on the molecular surface. The latter value, despite the contribution of C···Cl contacts to the Hirshfeld surface area is negligible (C_{CCl} = 1.9%), is explained by a minor proportion of chlorine atoms on the molecular surface (S_{Cl} = 6.5%), decreasing the value of R_{CCl} (1.9%). Abundant S_H proportion of hydrogen atoms on the molecular surface also explains the higher propensity of the H···S contacts for both structures (E_{SH} = 1.47 and 1.17 for **1** and **4**, respectively). Furthermore, the high S_H value of the structure of **1** is the reason that the H···O contacts are enriched (E_{OH} = 1.33). Interestingly, the C···C contacts in the structure of **1** are the most enriched ones (E_{CC} = 1.73), which is due to the negligible value R_{CC} (2.2%), though the contribution of C···C contacts to the Hirshfeld surface area in the structure of **1** is also very negligible (C_{CC} = 3.8%).

Contacts of the type H···N and C···O, found in the structure of **1**, and Cl···Cl, appeared in the structure of **4**, are very impoverished (Table 1).

Conclusions

In summary, we have demonstrated the synthesis of a new *N*-phosphorylated thiourea, 3-ClNHC(S)NHP(O)$(OPh)_2$ (**1**), by the addition of neat phosphorylisothiocyanate to neat 3-chloroaniline. The same reaction in non-dried CH_2Cl_2 or C_6H_6 leads to salt-like compounds $[3\text{-}ClC_6H_4NH_3]^+[NCS]^-$ (**2**) and $[3\text{-}ClC_6H_4NH_3]^+$-$[P(O)_2(OPh)_2]^-\cdot 0.5C_6H_6$ (**3·0.5C$_6$H$_6$**), respectively, while using non-dried acetone yields 1-(3-chlorophenyl)-4,4,6-trimethyl-3,4-dihydropyrimidine-2(1*H*)-thione (**4**). Dissolution of **1** in non-dried CH_2Cl_2, C_6H_6 or $Me_2C{=}O$ leads to the direct formation of **2**, **3·0.5C$_6$H$_6$** and **4**, respectively. It was established that thione **4** is most likely formed through the thiourea **1**-assisted aldol condensation of acetone leading to mesityl oxide. In turn the latter ketone interacts with **1** followed by its hydrolysis leading to **4**. Thus, thiourea **1** might be considered as a facile single source precursor for **4**. Further research using other ketones is in progress.

Hirshfeld surface analysis showed that the structures of both **1** and **4** are mainly characterized by H···H, H···C, H···Cl and H···S contacts as well as by H···O in the structure of **1**. The enrichment ratio, derived as the decomposition of the crystal contact surface between pairs of interacting chemical species, for **1** was found, as expected for the polar contacts, which are generally hydrogen bonds, to be significantly larger than unity for the contacts of the type H···O and H···S. A much larger than unity value was found for the enrichment ratio of the C···C contacts in the structure of **1**, which is due to extensive π···π stacking in the crystal packing. The enrichment ratio for **4** was found to be larger than unity for the contacts of the type H···C and, but with a lesser degree, H···Cl and H···S.

Experimental

General procedures

NMR spectra in acetone-d_6 were obtained on a Bruker Avance 300 MHz spectrometer at 25 °C. ^{1}H and ^{31}P{^{1}H} NMR spectra were recorded at 299.948, and 121.420 MHz, respectively. Chemical shifts are reported with reference to $SiMe_4$ (^{1}H) and 85% H_3PO_4 (^{31}P{^{1}H}). Elemental analyses were performed on a Thermoquest Flash EA 1112 Analyzer from CE Instruments.

Syntheses

All syntheses were performed in non-dried solvents under ambient conditions.

Synthesis of 1. Neat 3-chloroaniline (0.127 g, 1 mmol) was treated under vigorous stirring with neat $(PhO)_2P(O)NCS$ (0.321 g, 1.1 mmol). The dark yellow viscous oil formed was dissolved in Et_2O (20 mL). The resulting solution was filtered and left overnight. Colorless block-like crystals, suitable for X-ray analysis, were filtered off, washed with Et_2O (3 × 10 mL) and dried *in vacuo*. Yield: 0.394 g (94%). ^{1}H NMR, δ: 6.96–7.81 (m, 62H, C_6H_5 + C_6H_4), 10.97 (br. s, 3.3H, PNH), 12.24 (br. s, 1H, PNH), 13.72 (br. s, 3.5H, arylNH), 13.91 (br. s, 1.1H, arylNH) ppm. $^{31}P\{^1H\}$ NMR, δ: −7.9 (s, 1P), −10.5 (s, 3.6P) ppm. Anal. calc. for $C_{19}H_{16}ClN_2O_3PS$ (418.83): C, 54.49; H, 3.85; N, 6.69. Found: C, 54.61; H, 3.91; N, 6.74.

Synthesis of 2–4 (Path A). A solution of 3-chloroaniline (0.127 g, 1 mmol) in CH_2Cl_2, C_6H_6 or $Me_2C{=}O$ (10 mL) was treated under vigorous stirring with a solution of $(PhO)_2P(O)NCS$ (0.321 g, 1.1 mmol) in the same solvent (15 mL). The resulting solution was stirred for 2 h, filtered and left for slow evaporation at room temperature. Colorless plate-like crystals, suitable for X-ray analysis, were obtained after two-three days. Crystals were filtered off, washed with Et_2O (3 × 10 mL) and dried *in vacuo*.

2. Yield: 0.162 g (87%). ^{1}H NMR, δ: 7.21–7.38 (m, 4H, C_6H_4), 8.18 (br. s, 3H, NH_3) ppm. Anal. calc. for $C_7H_7ClN_2S$ (186.66): C, 45.04; H, 3.78; N, 15.01. Found: C, 45.13; H, 3.72; N, 15.12.

3·0.5(C_6H_6). Yield: 0.379 g (91%). ^{1}H NMR, δ: 6.90–7.45 (m, 17H, C_6H_6 + C_6H_5 + C_6H_4), 8.13 (br. s, 3H, NH_3) ppm. $^{31}P\{^1H\}$ NMR, δ: −11.7 ppm. Anal. calc. for $C_{21}H_{20}ClNO_4P$ (416.82): C, 60.51; H, 4.84; N, 3.36. Found: C, 60.63; H, 4.77; N, 3.28.

4. Yield: 0.162 g (84%). ^{1}H NMR, δ: 1.39 (s, 6H, $C(CH_3)_2$), 1.54 (d, $^4J_{H,H}$ = 1.1 Hz, 3H, CH═CCH_3), 5.00 (q, $^4J_{H,H}$ = 1.1 Hz, 1H, CH═CCH_3), 7.17–7.42 (m, 4H, C_6H_4), 7.90 (br. s, 1H, NH) ppm. Anal. calc. for $C_{13}H_{15}ClN_2S$ (266.79): C, 58.53; H, 5.67; N, 10.50. Found: C, 58.65; H, 5.61; N, 10.42.

Synthesis of 2–4 (Path B). A powdered sample of **1** (0.105 g, 0.25 mmol) was dissolved in CH_2Cl_2, C_6H_6 or $Me_2C{=}O$ (15 mL). The resulting solution was stirred for 2 h and left overnight. Colorless plate-like crystals, suitable for X-ray analysis, were obtained after one-two days. Crystals were filtered off, washed with Et_2O (3 × 10 mL) and dried *in vacuo*.

2. Yield: 0.045 g (96%).

3·0.5(C_6H_6). Yield: 0.098 g (94%).

4. Yield: 0.060 g (90%).

Single crystal X-ray diffraction

The X-ray data of **1–4**, obtained *via* Path A, were collected at 150(2) (**1** and **2**) and 297(2) 150(2) (**3·0.5(C_6H_6)** and **4**) K on a Mar345 image plate detector using Mo-K_α radiation (Xenocs Fox3D mirror). The data were integrated with the CrysAlisPro software.[17] The implemented empirical absorption correction was applied. The structures were solved by SHELXS[18] and refined by full-matrix least squares on $|F^2|$, using SHELXL2014/7.[19] Non-hydrogen atoms were anisotropically refined and the hydrogen atoms were placed on calculated positions in the riding mode with temperature factors fixed at 1.2 times U_{eq} of the parent atoms. Figures were generated using the program Mercury.[20]

Crystal data for 1. $C_{19}H_{16}ClN_2O_3PS$, M_r = 418.82 g mol^{-1}, monoclinic, space group $P2_1/c$, a = 17.7272(3) Å, b = 10.9714(2) Å, c = 10.2468(2) Å, β = 97.6257(19)°, V = 1975.30(6) Å^3, Z = 4, ρ = 1.408 g cm^{-3}, μ(Mo-Kα) = 0.402 mm^{-1}, reflections: 11 779 collected, 3630 unique, R_{int} = 0.024, R_1(all) = 0.0387, wR_2(all) = 0.0951.

Crystal data for 2. C_6H_7ClN, CNS; M_r = 186.66 g mol^{-1}, monoclinic, space group $P2_1/c$, a = 15.742(4) Å, b = 7.7102(9) Å, c = 7.0694(12) Å, β = 99.36(2)°, V = 846.6(3) Å^3, Z = 4, ρ = 1.464 g cm^{-3}, μ(Mo-Kα) = 0.630 mm^{-1}, reflections: 5161 collected, 1523 unique, R_{int} = 0.076, R_1(all) = 0.0928, wR_2(all) = 0.2192.

Crystal data for 3·0.5(C_6H_6). $C_{12}H_{10}O_4P$, C_6H_7ClN, 0.5(C_6H_6); M_r = 416.80 g mol^{-1}, triclinic, space group $P\bar{1}$, a = 6.7856(6) Å, b = 11.797(5) Å, c = 15.113(4) Å, α = 67.80(3), β = 80.388(17), γ = 74.82(2)°, V = 1077.9(6) Å^3, Z = 2, ρ = 1.284 g cm^{-3}, μ(Mo-Kα) = 0.277 mm^{-1}, reflections: 12 856 collected, 3723 unique, R_{int} = 0.035, R_1(all) = 0.0471, wR_2(all) = 0.1417.

Crystal data for 4. $C_{13}H_{15}ClN_2S$, M_r = 266.78 g mol^{-1}, monoclinic, space group $P2_1/c$, a = 8.4353(4) Å, b = 14.9782(9) Å, c = 11.5168(8) Å, β = 104.453(6)°, V = 1409.05(15) Å^3, Z = 4, ρ = 1.258 g cm^{-3}, μ(Mo-Kα) = 0.400 mm^{-1}, reflections: 9066 collected, 2524 unique, R_{int} = 0.044, R_1(all) = 0.0552, wR_2(all) = 0.1878.

CCDC 1423371 (**1**), 1423372 (**2**), 1423373 (**3**) and 1423374 (**4**) contain the supplementary crystallographic data.

Acknowledgements

M. G. Babashkina and D. A. Safin thank WBI (Belgium) for the post-doctoral positions. This work was partly supported by FNRS (Belgium).

References

1 (*a*) F. D. Sokolov, D. A. Safin, N. G. Zabirov, A. Yu. Verat, V. V. Brusko, D. B. Krivolapov, E. V. Mironova and I. A. Litvinov, *Polyhedron*, 2006, **25**, 3611; (*b*) D. A. Safin, M. G. Babashkina, F. D. Sokolov, N. G. Zabirov, J. Galezowska and H. Kozlowski, *Polyhedron*, 2007, **26**, 1113; (*c*) D. A. Safin, F. D. Sokolov, Ł. Szyrwiel, M. G. Babashkina, T. R. Gimadiev, F. E. Hahn, H. Kozlowski, D. B. Krivolapov and I. A. Litvinov, *Polyhedron*, 2008, **27**, 2271; (*d*) F. D. Sokolov, D. A. Safin, M. Bolte, E. R. Shakirova and M. G. Babashkina, *Polyhedron*, 2008, **27**, 3141; (*e*) D. A. Safin, F. D. Sokolov, T. R. Gimadiev, V. V. Brusko, M. G. Babashkina, D. R. Chubukaeva, D. B. Krivolapov and I. A. Litvinov, *Z. Anorg. Allg. Chem.*, 2008, **634**, 967; (*f*) D. A. Safin, M. G. Babashkina, M. Bolte and A. Klein, *Polyhedron*, 2009, **28**, 1403; (*g*) R. C. Luckay, X. Sheng, C. E. Strasser, H. G. Raubenheimer, D. A. Safin, M. G. Babashkina and A. Klein, *Dalton Trans.*, 2009, 8227; (*h*) D. A. Safin, M. G. Babashkina and A. Klein, *Croat. Chem. Acta*, 2010, **83**, 353; (*i*) D. A. Safin, M. G. Babashkina, M. Bolte and A. Klein, *Heteroat. Chem.*, 2010, **21**, 343; (*j*) M. G. Babashkina and D. A. Safin, *Phosphorus, Sulfur Silicon Relat. Elem.*, 2010, **185**, 1437; (*k*) M. G. Babashkina,

E. R. Shakirova, D. A. Safin, F. D. Sokolov, A. Klein, Ł. Szyrwiel, M. Kubiak, H. Kozlowski and D. B. Krivolapov, *Z. Anorg. Allg. Chem.*, 2010, **636**, 2626; (*l*) M. G. Babashkina, D. A. Safin, A. Klein and M. Bolte, *Eur. J. Inorg. Chem.*, 2010, 4018; (*m*) D. A. Safin, M. G. Babashkina, M. Bolte and M. Köckerling, *Inorg. Chim. Acta*, 2011, **370**, 59; (*n*) M. G. Babashkina, D. A. Safin, M. Srebro, P. Kubisiak, M. P. Mitoraj, M. Bolte and Y. Garcia, *CrystEngComm*, 2011, **13**, 5321; (*o*) M. G. Babashkina, D. A. Safin, K. Robeyns, A. Brzuszkiewicz, H. Kozlowski and Y. Garcia, *CrystEngComm*, 2012, **14**, 1324; (*p*) M. G. Babashkina, D. A. Safin and Y. Garcia, *Polyhedron*, 2012, **33**, 114; (*q*) M. G. Babashkina, D. A. Safin, K. Robeyns and Y. Garcia, *Dalton Trans.*, 2012, **41**, 1451; (*r*) D. A. Safin, M. G. Babashkina, A. P. Railliet, N. A. Tumanov, K. Robeyns, E. Devlin, Y. Sanakis, Y. Filinchuk and Y. Garcia, *Dalton Trans.*, 2013, **42**, 5532; (*s*) D. A. Safin, M. G. Babashkina, K. Robeyns, M. P. Mitoraj, P. Kubisiak, M. Brela and Y. Garcia, *CrystEngComm*, 2013, **15**, 7845; (*t*) D. A. Safin, M. G. Babashkina, M. Bolte and Y. Garcia, *Polyhedron*, 2013, **63**, 133; (*u*) D. A. Safin, M. G. Babashkina, K. Robeyns, M. Bolte and Y. Garcia, *CrystEngComm*, 2014, **16**, 7053; (*v*) D. A. Safin, M. G. Babashkina, P. Kubisiak, M. P. Mitoraj, C. S. Le Duff, K. Robeyns and Y. Garcia, *Eur. J. Inorg. Chem.*, 2014, 5522; (*w*) M. G. Babashkina, D. A. Safin, K. Robeyns and Y. Garcia, *Eur. J. Inorg. Chem.*, 2015, 1160.

2 (*a*) I. Ugi, A. Dömling and W. Hörl, *Endeavour*, 1994, **18**, 115; (*b*) R. W. Armstrong, A. P. Combs, P. A. Tempest, S. D. Brown and T. A. Keating, *Acc. Chem. Res.*, 1996, **29**, 123; (*c*) L. F. Tietze and M. E. Lieb, *Curr. Opin. Chem. Biol.*, 1998, **2**, 363; (*d*) A. Dömling, *Comb. Chem. High Throughput Screening*, 1998, **1**, 1; (*e*) S. L. Dax, J. J. McNally and M. A. Youngman, *Curr. Med. Chem.*, 1999, **6**, 255.

3 (*a*) M. Plunkett and J. A. Ellman, *Sci. Am.*, 1997, **276**, 68; (*b*) S. L. Schreiber, *Science*, 2000, **287**, 1964.

4 P. Biginelli, *Gazz. Chim. Ital.*, 1893, **23**, 360.

5 C. O. Kappe, *Acc. Chem. Res.*, 2000, **33**, 879.

6 O. Alam, M. Imran and S. A. Khan, *Indian J. Heterocycl. Chem.*, 2005, **14**, 293.

7 S. N. Swamy, Basappa, B. S. Priya, B. Prabhuswamy, B. H. Doreswamy, J. S. Prasad and K. S. Rangappa, *Eur. J. Med. Chem.*, 2006, **41**, 531.

8 D. Sriram, P. Yogeeswari and R. V. Devakaram, *Bioorg. Med. Chem.*, 2006, **14**, 3113.

9 A. C. L. Leite, R. S. Lima, D. R. M. Moreira, M. V. O. Cardoso, A. C. G. Brito, L. M. F. Santos, M. Z. Hernandes, A. C. Kiperstok, R. S. Lima and M. B. P. Soares, *Bioorg. Med. Chem.*, 2006, **14**, 3749.

10 G. C. Rovnyak, S. D. Kimball, B. Beyer, G. Cucinotta, J. D. DiMarco, J. Gougoutas, A. Hedberg, M. Malley, J. P. McCarthy, R. Zhang and S. Moreland, *J. Med. Chem.*, 1995, **38**, 119.

11 F. D. Sokolov, V. V. Brusko, N. G. Zabirov and R. A. Cherkasov, *Curr. Org. Chem.*, 2006, **10**, 27.

12 M. A. Spackman and D. Jayatilaka, *CrystEngComm*, 2009, **11**, 19.

13 M. A. Spackman and J. J. McKinnon, *CrystEngComm*, 2002, **4**, 378.

14 S. K. Wolff, D. J. Grimwood, J. J. McKinnon, M. J. Turner, D. Jayatilaka and M. A. Spackman, *CrystalExplorer 3.1*, University of Western Australia, 2012.

15 For example: D. A. Safin, M. P. Mitoraj, K. Robeyns, Y. Filinchuk and C. M. L. Vande Velde, *Dalton Trans.*, 2015, **44**, 16824.

16 C. Jelsch, K. Ejsmont and L. Huder, *IUCrJ*, 2014, **1**, 119.

17 Rigaku Oxford Diffraction, *CrysAlisPro Software system, Version 1.171.37.31*, Rigaku Corporation, Oxford, UK, 2014.

18 G. M. Sheldrick, *Acta Crystallogr., Sect. A: Found. Crystallogr.*, 2008, **64**, 112.

19 G. M. Sheldrick, *SHELXL2014/7*, University of Göttingen, Germany, 2014.

20 I. J. Bruno, J. C. Cole, P. R. Edgington, M. Kessler, C. F. Macrae, P. McCabe, J. Pearson and R. Taylor, *Acta Crystallogr., Sect. B: Struct. Sci.*, 2002, **58**, 389.

